$MoSi_2$-Base Hybrid Composites For Aeroengine Applications

M. G. Hebsur
National Aeronautics and Space Administration
Glenn Research Center
Cleveland, Ohio 44135

Abstract

Addition of about 30 to 50 vol % of Si_3N_4 particulate to $MoSi_2$ improved low temperature accelerated oxidation resistance by forming a Si_2ON_2 protective scale and thereby eliminated catastrophic 'pest failure'. The Si_3N_4 addition also improved the high temperature creep strength by nearly five orders of magnitude, doubled the room temperature toughness, and significantly lowered the CTE of the $MoSi_2$ which eliminated matrix cracking in SCS-6 reinforced composites even after thermal cycling. The SCS-6 fiber reinforcement improved the room temperature fracture toughness by seven times and impact resistance by five times. The composite exhibited this excellent strength and toughness improvement up to 1673 K. More recently, tape casting was adopted as the preferred processing of $MoSi_2$-base composites due to improved fiber spacing, ability to use small diameter fibers, and for lower cost. Good strength and toughness values were also obtained with fine diameter Hi-Nicalon tow fibers. These hybrid composites remain competitive with ceramic matrix composites as a replacement for Ni-base superalloys in aircraft engine applications.

1. Introduction

The intermetallic compound $MoSi_2$ has long been known as a high-temperature material that has excellent oxidation resistance and electrical and thermal conductivity. Also, its low cost, high melting point (2296 K), relatively low density (6.2 versus 8 g/cc for current engine materials), and ease of machining make it an attractive structural material [1]. However, the use of $MoSi_2$ has been hindered due to the brittle nature of the material at low temperatures, inadequate creep resistance at high temperatures, accelerated ('pest') oxidation at temperatures near 773 K, and its relatively high coefficient of thermal expansion (CTE) compared to potential reinforcing fibers such as SiC. The CTE mismatch between the fiber and the matrix results in severe matrix cracking during thermal cycling.

In the last 15 years, an extensive amount of work has been carried out in efforts to improve the high-temperature properties of $MoSi_2$ by solid solution alloying, discontinuous reinforcement, and fiber reinforcement. Alloying with W or Re has improved high temperature creep strength [2]. Substantial improvements in strength have also been achieved by adding particulates, platelets or whiskers of SiC, TiB_2, and HfB_2. However, the effects of grain refinement may limit the creep strength of these types of composites. To date, $MoSi_2$ alloyed with W and containing 40 vol % SiC has achieved the best creep strength and is superior to superalloys, although is still not as good as the best monolithic ceramics. The addition of SiC whiskers has also yielded improvements in room temperature toughness. However, it appears that the strength and damage tolerance required for high-temperature aerospace applications can only be achieved by reinforcement with high-strength continuous fibers.

Maloney and Hecht [3] have done extensive work on the development of continuous fiber reinforced $MoSi_2$ base composites to achieve high-temperature creep resistance and room-temperature toughness. Candidate fibers consisted of ceramic fibers, such as SiC and single crystal Al_2O_3, and ductile Mo, and W alloy fibers. The refractory metal fibers increased both creep strength and fracture toughness, although reaction with the matrix was still a problem. The addition of about 40 vol % of SiC in the form of whiskers and particulate was used to lower the thermal expansion of the $MoSi_2$ base matrix. However, matrix cracking was still observed in an SCS-6 fiber reinforced composite even with the matrix containing up to 40 vol % SiC whiskers. This composite also suffered catastrophic pest attack at 773 K. Sapphire fiber reinforced composites showed no evidence of matrix cracking due to the good thermal expansion match between $MoSi_2$ and Al_2O_3. However, the strong fiber-matrix bond did not provide any toughness improvement.

The pesting phenomenon is caused by the formation of voluminous Mo oxides in the microcracks. During the accelerated oxidation, MoO_3 and SiO_2 are simultaneously formed in amounts determined by their concentrations in the intermetallic. The accelerated oxidation is a necessary, but not sufficient, condition for pesting. Recent improvements in the fabrication of $MoSi_2$ have led to materials with less porosity that are correspondingly less susceptible to pest attack. However, because of increased surface areas and fabrication complexities from incorporating reinforcement phases in $MoSi_2$-based composites, pesting of composite materials is still a major concern.

In earlier work [4] in the development of $MoSi_2$ suitable for SiC fiber reinforcement, it was found that the addition of about 30 to 50 vol % of Si_3N_4 particulate to $MoSi_2$ improved the low temperature accelerated oxidation resistance by forming a Si_2ON_2 protective scale and thereby eliminated catastrophic pest failure. The Si_3N_4 addition also improved the high temperature oxidation resistance and compressive strength. The brittle-to-ductile (BDTT) transition-temperature of $MoSi_2$-$30Si_3N_4$, measured in 4 point bending, was between 1173 and 1273 K. More importantly, the Si_3N_4 addition significantly lowered the CTE of the $MoSi_2$ and eliminated matrix cracking in SCS-6 reinforced composites even after thermal cycling [5].

These encouraging preliminary results led to a joint program for further composite development between Pratt and Whitney, the Office of Naval Research, and NASA Glenn. The overall technical direction of this long-range program is to develop $MoSi_2$-base composite systems for advanced aircraft engine applications as a competitor to both today's superalloys and other advanced materials, primarily ceramic matrix composites. A turbine blade outer air seal for Pratt and Whitney's ATEGG/JTD engine demonstrator was chosen as the first component upon which to focus. This paper briefly describes the progress made so far in developing, processing, and characterizing $MoSi_2$ base hybrid composites.

2. Experimental

Attrition milling of $MoSi_2$ and Si_3N_4 powder is the first step in composite processing. Several batches containing a mixture of commercially available $MoSi_2$ and either 30 or 50 vol % of Si_3N_4 were mechanically alloyed in a Union Process attritor. No densification aids were added to the $MoSi_2$-Si_3N_4 mixtures. The average mean particle size of the mixture after milling was 1.25±0.71 μm at 99 percent confidence. The $MoSi_2$-Si_3N_4 powder was consolidated into "matrix-only" plates 12-cm long × 5-cm wide × 0.3-cm thick, or a larger size of 18-cm long × 2.5-cm wide × 1.25-cm thick. The plates were consolidated by vacuum hot pressing to achieve about 60 percent density. Further consolidation of the hot pressed plate was achieved by hot isostatic pressing (HIP). Composite plates of various thickness consisting of 6, 12, or 54 plies of 30 vol % SCS-6, and coated Hi-Nicalon fibers having 0, 0/90 and 90 orientations in a $MoSi_2$-Si_3N_4 matrix were prepared by the powder cloth and tape casting techniques [6] respectively, and consolidated in the same manner as the material without fibers. The 2-step consolidation process enabled the use of a lower consolidation temperature than could be used if only hot pressing was performed. The two-step densification process resulted in fully dense material without excessive reaction or damage to the fibers.

From the consolidated material, ASTM standard specimens for several mechanical tests such as fracture toughness, tensile, impact and flexural creep were machined by electrodischarge machining (EDM) and grinding techniques. Tensile tests were conducted on 1.27×15 cm straight or dog bone-shaped specimens machined from 6 ply composite panels. Tests were performed in air between 230 and 1473 K at an initial strain rate of 1.4×10^{-3} sec^{-1}. Fracture toughness tests were measured on chevron notched bend specimens made from 12 ply composite panels, tested at a constant strain rate of 1.2×10^{-5} cm/min. ASTM full size Charpy V-notch impact specimens were machined from 54 ply composites and impact tests were conducted using a 356 J Tinus Olsen impact tester with Dynatrup instrumentation. Heating of the specimen was carried out using two oxypropane torches and the temperature was monitored using a laser pyrometer. Constant-stress flexural rupture tests were conducted on 6-mm wide × 4-mm deep × 50-mm long specimens of $MoSi_2$-$50Si_3N_4$ monolithic and fiber reinforced composites at 1473 K and 210 MPa in air. Detailed microstructural characterization of as-fabricated and tested specimens were carried out using standard optical and electron microscopic techniques.

3. Results and Discussion

Figure 1 shows the transverse microstructure of the as-fabricated $MoSi_2$-Si_3N_4/SCS-6 composite. A reaction zone around the fibers was generally less than 1 μm in thickness and resulted from reaction of the carbon layer to form SiC and Mo_5Si_3. Although the fiber distribution is not uniform, Fig. 1 indicates the absence of matrix cracking. The CTE measurements made on the $MoSi_2$-Si_3N_4 matrix-only plate and composites as compared with the monolithic constituents indicated that the addition of Si_3N_4 to $MoSi_2$ has effectively lowered the CTE of the matrix, achieving the desired result of eliminating matrix cracking. Furthermore, no cracks were found in either the matrix or the reaction zone even after 1000 thermal cycles between 1473 and 473 K. These results indicate that the use of Si_3N_4 was much more effective than similar attempts using SiC in lowering the CTE of $MoSi_2$ and in preventing cracking in the $MoSi_2$-base composites.

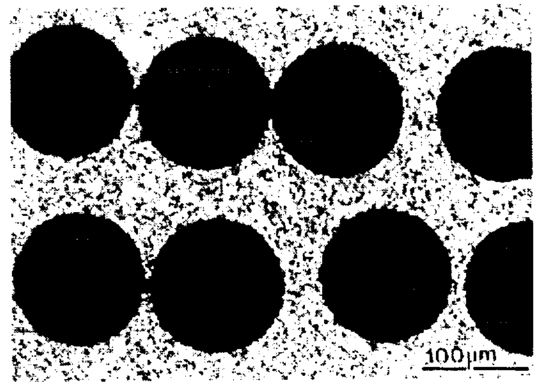

Figure 1.—SEM-BSE image of powder cloth fabricated SCS-6/$MoSi_2$-$30Si_3N_4$ hybrid composites.

Figure 2 shows the load verses time plot for SCS-6 $MoSi_2$-$30Si_3N_4$ monolithic chevron notched 4 point bend specimens tested at room temperature. The composite specimen did not break even after testing for 2 hr. The apparent critical stress intensity factor, K_q [7] calculated from the maximum load data was greater than 35 MPa√m indicating that the hybrid composite specimen was 7 times

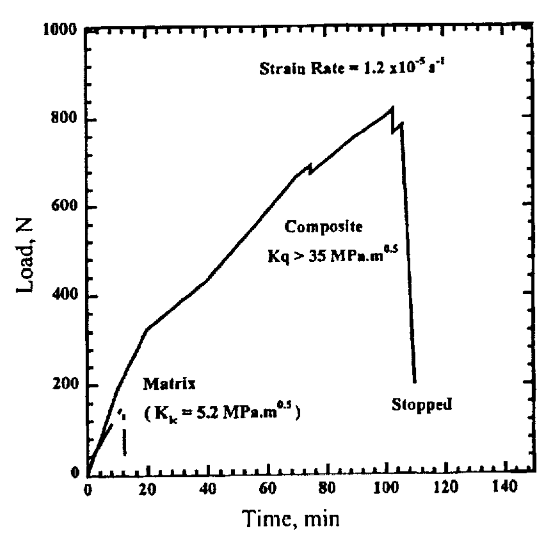

Figure 2.—Load-time curves from chevron notched 4 point bend tested SCS-6/$MoSi_2$-$50Si_3N_4$ and $MoSi_2$-$50Si_3N_4$ specimen at room temperature.

tougher than the monolithic material. The toughness of the hybrid composite also increased with temperature reaching as high as 65 MPa$\sqrt{m}$, at 1673 K in argon atmosphere.

Room temperature tensile stress strain data for SCS-6/$MoSi_2$-Si_3N_4, indicated composite-like behavior; and three distinct regions, an initial linear region, followed by a nonlinear region and a second linear region. The nonlinear region is due to the matrix cracking normal to the loading direction. The second linear region is controlled by fiber bundle strength. Figure 3 shows the temperature dependence of ultimate tensile strength, along with the data from competitive materials, namely single crystal PWA1480 [8], and SCS-6/reaction bonded silicon nitride (RBSN) [9]. PWA 1480 exhibits higher tensile strength than both $MoSi_2$-base and RBSN-base composites between room temperature and 1273 K however, PWA 1480 is almost 3 times denser than both composites, and hence is at a disadvantage on a specific strength basis. However, SiC-SiC composites retain their strengths beyond 1473 K. Figure 3 also shows the tensile strength data for the SCS-6 fibers, re-emphasizing the fiber-dominated behavior of the composites. The $MoSi_2$-base composites also exhibited elastic modulus values of ~290 to 200 GPa between RT and 1473 K, which were substantially higher than comparable CMCs over these temperatures. Unlike most CMC's, which have as much as 20 percent porosity, these

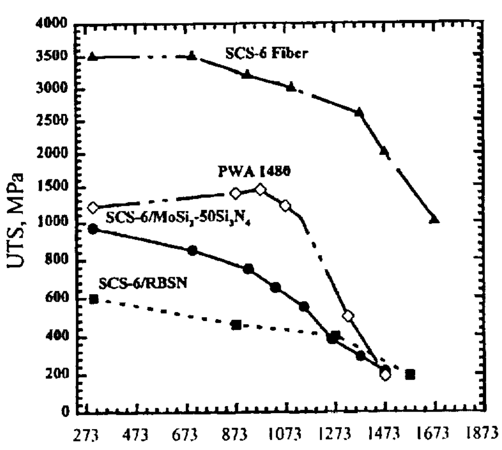

Figure 3.—Temperature dependence of ultimate tensile strength of SCS-6/$MoSi_2$-$50Si_3N_4$ base composites compared with other materials.

$MoSi_2$-base composites are fully dense and hence exhibit higher modulus.

Aircraft engine components require sufficient toughness to resist manufacturing defects, assembly damage, stress concentrations at notches, and foreign and domestic object damage. Consultation with engine company designers indicated a strong desire for not only fracture toughness but more importantly, impact resistance to be measured before they would seriously consider these types of composites. The Charpy V-notch (CVN) test was chosen to assess impact resistance based on the engine designer's desire to use a relative ranking against more familiar materials, rather than a formal design requirement.

CVN impact tests were conducted on full size specimens of $MoSi_2$-$50Si_3N_4$ matrix and SCS-6 [0] and [0/90] oriented $MoSi_2$-$50Si_3N_4$ hybrid composites between room temperature and 1673 K in air. The hybrid composite in [0] orientation exhibited the highest peak force values, followed by the cross-plied and finally the monolithic material. At 1673 K, the peak force values for all three materials were higher than their corresponding values at room temperature. The hybrid composite exhibited a gradual, stepwise decrease in load after the peak force was achieved. This indicates substantial energy absorption during crack propagation, and was especially pronounced in the [0] orientation.

Figure 4 shows the temperature dependence of CVN energy for $MoSi_2$-base materials compared with other potential materials such as superalloys, and ceramics. The CVN energy for both the monolithic $MoSi_2$-$50Si_3N_4$ and the hybrid composites increased with increase in temperature. The fiber reinforcement in [0] orientation increased the impact resistance by 5 times and in [0/90] orientation nearly two times. The CVN energy of SCS-6/$MoSi_2$-$50Si_3N_4$ was comparable to the cast superalloy B-1900 but substantially lower than the wrought superalloy Hastelloy X. The CVN energy of $MoSi_2$-$50Si_3N_4$ monolithic was comparable to Mo alloys and in-situ toughened Si_3N_4 (As-800) and was far superior to NiAl, and monolithic hot pressed Si_3N_4, and SiC. Unlike $MoSi_2$-$50Si_3N_4$ which shows increased CVN energy with temperature, SiC shows a slight decrease of CVN energy with temperature (beyond 1273 K), the AS-800 shows a constant CVN energy between –573 and 1673 K. The monolithic SiC shows a slight decrease of CVN energy with temperature. This is probably due to the degradation caused by densification aids used with SiC. SEM examination of impact tested SCS-6/$MoSi_2$-50 Si_3N_4 showed substantial fiber pullout in [0] orientation and limited fiber pullout in [0/90] oriented specimens at all temperatures.

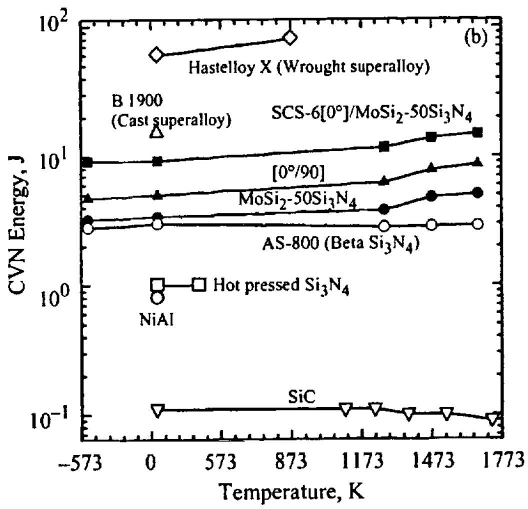

Figure 4.—CVN energy versus temperature plot for $MoSi_2$-base composites compared with other materials.

3.1 Advanced Processing and Fibers for Low Cost and Complex Shaped $MoSi_2$-Base Composites

Most of the attractive strength and toughness values reported so far were achieved with composites reinforced with SCS-6 fibers made by Textron, Inc. This large diameter (145 μm) fiber was designed primarily for Ti-based composites. This fiber does not have adequate creep strength at the highest temperatures envisioned for $MoSi_2$ and is too large to be bent around the sharp radii needed to make complex shapes. However, it is easy to infiltrate matrix powders between these fibers, thus enabling composites to be fabricated routinely. This ease in fabrication was meant to be exploited by further characterization of key properties such as creep resistance, transverse properties, and performance of the composite in an engine test bed. However, finer diameter fibers are preferred on a cost, shape making, creep resistance, and toughness basis. Hi-Nicalon is the best currently available fiber, although Dow Corning's Sylramic® fiber, developed for the High Speed Civil Transport program, is also appropriate for this $MoSi_2$-Si_3N_4 matrix. A transition in effort to Hi-Nicalon fibers was therefore investigated, first using tow fibers, (i.e., strings of ~500 individual filaments that are spread out, wound on a drum and then infiltrated with matrix powder) and ultimately woven cloth (i.e., the tows are woven into two or three dimensional architectures before matrix infiltration).

In earlier studies, the powder cloth technique was used to produce SiC continuous fiber reinforced $MoSi_2$-base composites. The powder cloth process is labor intensive and cannot always produce a uniform fiber distribution. Melt infiltration and chemical vapor infiltration are popular methods for processing of CMC's because of the potential for making complex shapes and lower cost, but they are limited to thickness on the order of 5 mm, because segregation and porosity problems are aggravated in thick specimens. Tape casting was therefore adopted as a powder metallurgy method for composite fabrication. Initially, several tape casting trials of $MoSi_2.Si_3N_4$ were carried out to optimize various parameters such as particle size, type and amount of binder and solvent, flow behavior of the slurry, and binder burn-out cycle. A 54-ply composite of SCS-6/$MoSi_2$-Si_3N_4 was successfully fabricated by tape casting followed by the standard hot press plus HIP consolidation. Composites with small diameter fibers such as SCS-9 (75μm) and coated Hi-Nicalon (18 to 20 μm) were also successfully fabricated. Figure 5 illustrates the range in fiber diameters in this study. Note also the improvement in fiber spacing control between Figs. 5(a) and (b), achieved by switching from powder cloth to tape casting. Figure 6 shows efficient spreading of the

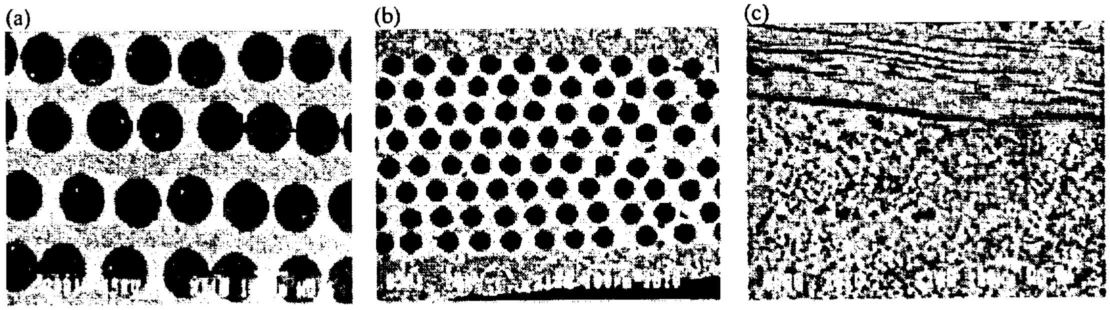

Figure 5.—SEM micrographs of SiC/$MoSi_2$-Si_3N_4 showing wide range of fiber diameters. (a) 140 μm SCS-6 fibers in matrix produced by powder cloth. (b) Same material as (a) but tape cast. (c) Hi-Nicalon fibers.

fiber tows and infiltration of $MoSi_2.Si_3N_4$ powder particles. Although there is still some heterogeneity in the fiber distribution, this microstructure is among the best we have seen on any other study using fine diameter fibers.

Interfacial coatings play a very important role in fiber reinforced composites, and the Hi-Nicalon tow fibers must be coated before compositing. Interfacial coatings that have proven successful in CMC's have been adopted for use with $MoSi_2$. To date, only carbon or BN have been able to provide the correct level of interfacial bonding required for toughening, but they both exhibit poor environmental resistance. Therefore, a protective coating of SiC or Si_3N_4 is required as a second layer on top of the debonding layer. Unfortunately, the coating technology for fine diameter tows has still not matured to the state where smooth, crack free and uniformly thick coatings can be produced. This immaturity is also reflected in the high cost and limited facilities nationally available for coating. Therefore, only limited mechanical properties have been generated with these fibers.

Figure 7 shows the influence of fiber diameter and architecture on flexural stress rupture at 1473 K/210 MPa in air. This figure clearly indicates the limited improvement with large diameter fibers and the more than 4 orders of magnitude improvement with fine diameter fiber [0/90 oriented] in stress rupture lives compared to the monolithic material. SEM of the stress ruptured Hi-Nicalon$_{[0/90]}$/ $MoSi_2$-Si_3N_4 composite revealed substantial fiber pull out on the tension side of the specimen.

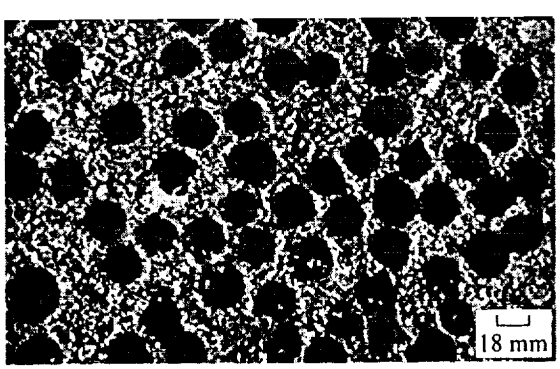

Figure 6.—SEM-SE image of BN/SiC coated Hi-Nicalon/$MoSi_2$-Si_3N_4 hybrid composite showing good fiber spreading and matrix infiltration.

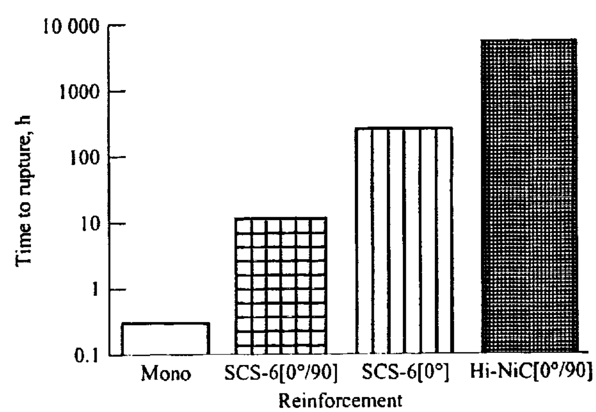

Figure 7.—Influence of SiC fiber diameter and orientation on flexural stress rupture of $MoSi_2$-$50Si_3N_4$ at 1473 °K/ 210 MPa.

3.2 Engine Testing of Hi-Nicalon/$MoSi_2$-Si_3N_4 Hybrid Composite

Encouraged by the preliminary results on mechanical behavior of the hybrid composite, it was decided to test this material in the aggressive environment of a gas turbine engine. Two panels of the BN/Si_3N_4 coated Hi-Nicalon$_{[0/90]}$ / $MoSi_2$-50Si_3N_4 hybrid composite, ~12-cm long × 6-cm wide × 0.6-cm thick were fabricated by tape casting and hot pressing techniques. From the consolidated panels, two engine test coupons were made according to Pratt and Whitney's design specification. After machining, the surfaces of these coupons were coated with 2 μm thick SiC by chemical vapor deposition (CVD) to protect the exposed fibers from environmental degradation. The coupons were tested in Pratt and Whitney's demonstrator engine. The test coupons with all instrumentation were placed behind the high pressure turbine blades in the engine. A small amount of clamping was used to hold the test coupon in place. One surface of the test coupons was facing the jet fueled flame, which reached ~1473 K and produced a thermal gradient of about 873 K between the exposed (front) and unexposed (back) surfaces. This hybrid composite performed significantly better than a SiC whisker reinforced $MoSi_2$, which developed several cracks within the first few cycles. The composite was removed after 15 cycles and post-test examination did not reveal any surface or matrix cracking [10].

Conclusions

$MoSi_2$-base hybrid composites remain competitive with state-of art ceramics as a replacement for superalloys in jet engines.

Acknowledgments

The author would like to acknowledge financial support from the Office of the Naval Research, Pratt & Whitney Aircraft, West Palm Beach, Florida and NASA Glenn Research Center, Cleveland, Ohio.

References

1. Vasudevan A K, and Petrovic J J, High Temperature Silicides, Ed. by Vasudevan A K and Petrovic J J, North Holland, New York (1992) pp. 1–17.
2. Petrovic J J, and Honnell R E, Cerm. Eng. Soc. Proc., 11 (1990) pp. 734–744.
3. Maloney M J, and Hecht R J, High Temperature Silicides, Ed., Vasudevan A K, and Petrovic J J, North Holland, New York (1992) pp. 19–31.
4. Hebsur M G, Intermetallic Composites III, Ed. By Graves J A, Bowman R R, and Lewandowski J J, MRS Proc., vol. 350 (1994) Pittsburgh, Pennsylvania, pp. 177–182.
5. Hebsur M G, "Pest resistant $MoSi_2$ materials and method of making" U.S. Patent, # 5,429,997 (1995).
6. Pickens J W, NASA TM–102060, (1989) NASA GRC, Cleveland, Ohio.
7. Blum I J, Eng. Fract. Mech., (1975) pp. 593–604.
8. Hebsur M G, and Miner R V, NASA TM–88950 (1987) NASA GRC Cleveland, Ohio.
9. Bhatt R T, NASA CP–10039, (1989) pp. 57–1–13 NASA GRC Cleveland, Ohio.
10. Hebsur M G, Materials Science and Engineering A 261 (1999) pp. 24–37.